The International Journal of Engineering and Science (IJES)
ISSN (e): 2319 – 1813 ISSN (p): 23-19 – 1805
|| Pages || PP 41-45 || 2020 ||

# CFD study of the effect of impeller clearance on the turbulence characteristics of the baffled stirred tank reactors

Devarajan Krishna Iyer[1], Ajey Kumar Patel[2]
[1,2]*Department of Civil Engineering, National Institute of Technology Warangal, Telangana, India*
*Corresponding Author:Ajey Kumar Patel*

----------***ABSTRACT***----------
*The present study investigates the flow patterns and turbulence characteristics in a baffled reactor stirred by six-bladed Rushton Turbine (RT) placed at 1/3rd and 1/9th height of the tank above its bottom surface using the Computational Fluid Dynamics (CFD) approach. The well-known double loop to single loop flow pattern transition and the associated reduction in the power number were accurately predicted using the steady state Multiple Reference Frame (MRF) impeller modelling scheme along with the standard $k-\varepsilon$ turbulence model closure. The substantial reduction in the characteristics of trailing vortices (size, strength and coherency) with the decrease in the impeller clearance leads to the formation of weaker wake region behind the blades. The weak entrainment of the wake reduces the pressure drag and torque associated with the rotating impeller which in turn decreases the impeller power number. Although, the RT located close to the tank bottom develops weaker discharge stream, the additional strong vortices generated below the impeller centre-plane increases the turbulent action near the bottom surface of the tank. The differences in the flow instabilities may be the likely reason for the observed flow pattern transition and this aspect needs detailed investigations using the advanced experimental and CFD methods in the near future.*

***KEYWORDS;-****Stirred tank reactor, Turbulent Flow, Impeller clearance, Flow pattern transition*

## I. INTRODUCTION

The stirred reactors with RT impeller placed near the bottom surface develop single re-circulation pattern suitable for the solid-liquid suspension processes and pump-mix mixers present in the nuclear industry at a lesser power consumption [1]. The critical ranges of impeller clearance (height of the impeller above the bottom surface of the tank) have been determined by several researchers [2-5] using the experimental as well as computational approaches below which the standard double loop pattern changes into single loop pattern with abrupt decrease in the power number. Further studies have been conducted to analyze the sensitivity of the critical ranges of impeller clearance towards the various reactors parameters. The rotational speed of the impeller [6], diameter of the vessel, physical properties of the fluid as well as the particle have insignificant influence on the critical ranges of impeller clearance under turbulent conditions [4] while the larger diameter of the impeller reduces the same for the effective flow pattern transition [1]. Unfortunately, less interest has been attributed till date in explaining the reasons behind these flow field variations as the impeller position is shifted near the bottom of the vessel. Thus the present study investigates the mechanism behind the reduction in the power number as the impeller clearance is reduced towards the bottom of the tank using the steady state CFD modelling approach. The steady state CFD approach was found to be suitable for modelling the complex flow pattern transitions and the allied flow field variables at a lower computational cost as compared to the unsteady approaches [7].

## II. STIRRED TANK CONFIGURATIONS AND COMPUTATIONAL METHODOLOGY

The baffled vessel agitated by RT impeller placed at one-third height of the tank (H/3) as well as one-ninth height of the tank (H/9) from the bottom surface were numerically simulated. The former standard configuration of the vessel is denoted as Std-C and the latter configuration is represented as Low-C respectively hereafter. The various dimensions of the tank, baffles and the impeller were same as that used by Wu and Patterson, 1989 [8]. The water was used as the working fluid and the impeller was rotated at a speed (N) of 200 rpm to generate the turbulent flow conditions corresponding to a Reynolds number of 29,000. The hybrid grids were developed for both the configurations by providing tetrahedral elements near the impeller region and hexahedral elements in the rest of the regions using the ANSYS Meshing tool. The steady state three dimensional Reynolds Averaged Navier Stokes (RANS) equations with standard k-ε turbulence model closure [9] were solved using the commercial ANSYS 17.0 software founded on the finite volume approach. The impeller rotation was modelled using the Multiple Reference Frame (MRF) technique [10] by properly coupling the flow fields solved in a rotating reference frame near the impeller region and in a stationary reference frame

in the other regions at the interface separating both the regions. The tank walls, baffle walls and the impeller parts were considered as no-slip boundaries along with the standard wall function for modelling the viscous flow [9] close to the boundaries. The tank top was treated using the symmetry boundary condition. The SIMPLE pressure-velocity coupling scheme was used to couple the Reynolds continuity and momentum equations and the second order upwind scheme was used to discretize the resulting equations. The simulations were considered as converged when the residuals of the flow variables and the volume integrated turbulent dissipation rate were dropped below $10^{-6}$. The simulations were conducted in a workstation having double precision 64 bit Intel (R) Xeon (R) E5-1620 3.6 GHz processor.

## III. GRID INDEPENDENCE STUDY

The grid independence study of the critical flow variables such as power number from impeller torque (Npt) and power number from turbulent dissipation rate ($N_{pe}$) associated with both the clearances were conducted by successively refining the tetrahedral elements enclosing the impeller so as to generate three computational grids viz. coarse, medium and fine respectively. The grid refinement factor between the coarse, medium and fine grids of both the impeller clearances were more than 1.311 and the respective fine grids have 83×66 tetrahedral elements in the horizontal as well as vertical directions of the blades leading to $6.7\times10^6$ elements in the entire tank volume. The variation of $N_{pt}$ and $N_{pe}$ with the grid resolution for the Std-C as well as Low-C are shown in the Figures 1(a) and 1(b) respectively. The predictions of $N_{pt}$ were properly converged at the fine grids of both the impeller clearances as the relative deviations of the same between the medium and fine grids were less than 1%. Also, the relative variations of $N_{pe}$ between the medium and fine grids of Std-C and Low-C were less than 8% indicating adequate convergence of the same with the respective fine grids. Further, the smaller relative difference (<8%) between $N_{pt}$ and $N_{pe}$ related with the fine grids of both the impeller clearances represent the consistency of standard k-ε turbulence model in predicting the turbulent quantities [12]. Due to the appropriate convergence of $N_{pt}$ and $N_{pe}$ with the fine grids of both the geometries, the respective results were validated with the classic experimental results obtained by the various researchers as shown in the Figures 1(a) and 1(b) respectively. The accurate predictions of $N_{pt}$ were obtained for both the impeller clearances as the relative deviations of the same with the standard results of Bates et al., 1963 [13] and Zhu et al., 2019 [1] were around 5.5%. The double re-circulation loop pattern related with the Std-C as well as the single re-circulation loop pattern linked with the Low-C were properly developed as shown in the Fig. 2. Also, weaker secondary circulation loops were generated near the top of the tank for the Low-C as indicated by Montante et al., 2001 [7]. Further, the drop in the $N_{pt}$ from Std-C to Low-C is 35.5% which is close to that obtained by Zhu et al., 2019 [1]. The Std-C and Low-C under predict the $N_{pe}$ by 15% as well as 11% may be due to the limitations of the standard k-ε turbulence model in predicting the turbulent quantities [14].

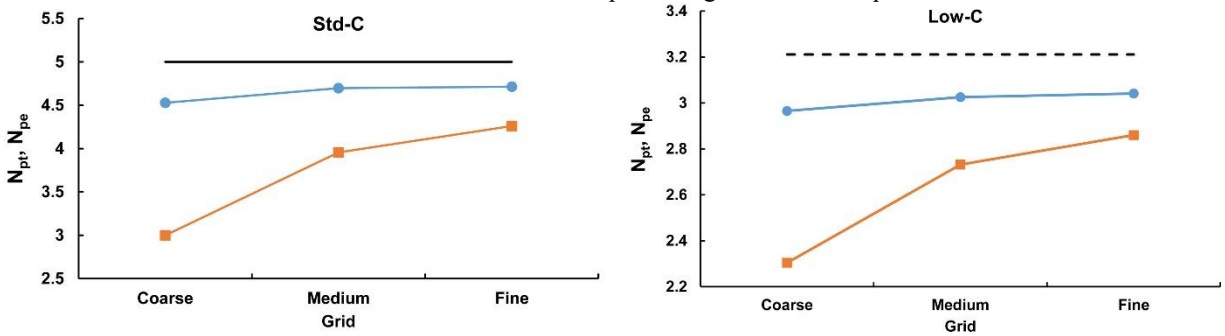


**Fig. 1. Variation of $N_{pt}$ and $N_{pe}$ with grid resolution for (a) Std-C and (b) Low-C**
**$N_{pt}$, $N_{pe}$, ——— : Bates et al., 1963 [13], – – : Zhu et al., 2019 [1]**

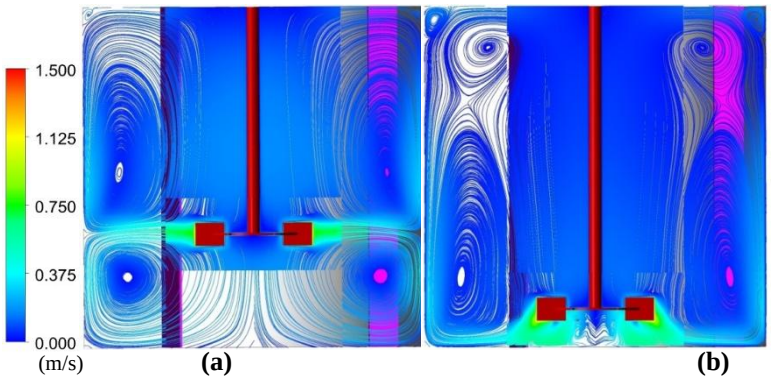


**Fig. 2. Re-circulation patterns of (a) Std-C and (b) Low-C in the mid-baffle plane**

## IV. RESULTS AND DISCUSSION

The characteristics of trailing vortices were studied using the contours of Q-criterion [15] as well as the axial profiles of normalized turbulence intensity ($U_{ti}/U_{tip}$) and turbulent dissipation rate ($e/N^3D^2$) at various angular distances behind the blades since the discharge stream is mainly composed of these periodic motions [16]. The $U_{tip}$ indicates the impeller tip velocity, D is the diameter of the impeller and w is the height of the blades. The axial profiles of turbulence parameters were plotted along a line connecting the vortex cores which were determined using the 'maximum vorticity magnitude' method [16]. The axial distance (z) is positive above the impeller centre-plane and negative below the impeller centre-plane.

Based on the contours of Q-criterion at various horizontal planes above and below the impeller centre-plane as exhibited in the Figures 3 and 4, the following inferences were derived. The trailing vortices associated with the Std-C are large and spread radially as well as azimuthally behind the impeller blades to larger extents. On the other hand, the trailing vortices linked with the Low-C are small and extend only to a small region behind the blades. Thus, the trailing vortices linked with the Std-C are more strong and coherent as compared to the Low-C. Although, the upper and lower trailing vortices disappear after certain angular distance behind the blades for Low-C, additional strong vortices which aren't attached to the impeller blades can be seen below the impeller centre-plane (Fig. 4(b)). A striking increase in the turbulence intensity as well as turbulent dissipation rate is also noticeable with the Std-C at various angular distances behind the blades in comparison with the Low-C as shown in the Fig. 5. Both the clearances developed highest magnitudes of turbulence parameters in an axial plane 10º behind the blades (Figures 5(a) & 5(d)) which reduces with further increase in the angular distance behind the blades. But the rate of decrease of turbulence parameters with the angular distance behind the blades is much higher for the Low-C as compared to the Std-C (Fig. 5). These flow features indicate that the Std-C develops larger, stronger and coherent trailing vortex structures as compared to the Low-C resulting in the formation of stronger and energetic flow separation region behind the blades. This in turn reduces the base pressure behind the blades and increases the pressure drag around the impeller [17]. The rise in the pressure drag increases the torque of the rotating impeller leading to higher $N_{pt}$ associated with the Std-C as compared to the Low-C.

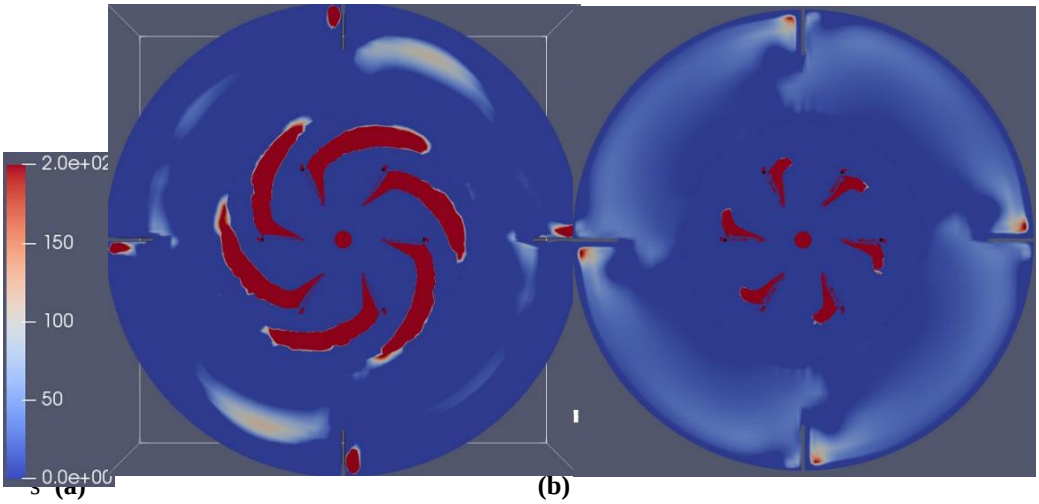


**Fig. 3. Contours of Q-criterion along a horizontal plane at 2z/w=0.97 for (a) Std-C and (b) Low-C**

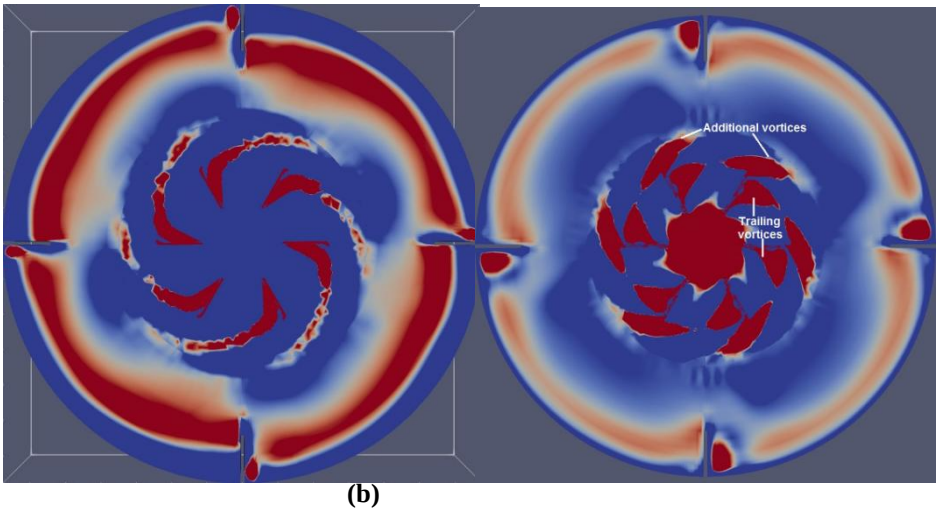


**(a)** **(b)**

**Fig. 4. Contours of Q-criterion along a horizontal plane at 2z/w=-1 for (a) Std-C and (b) Low-C**

The intense turbulent action near the bottom surface of the tank associated with the Low-C is due to the generation of additional strong vortices (Fig. 4(b)) since the turbulent characteristics and trailing vortices are weaker below the impeller centre-plane (Fig. 5). These vortices grow in size and angular extents below the impeller centre-plane. The main reason behind the double loop to single loop flow pattern transition from the Std-C to Low-C may be connected to the differences in the flow instabilities linked with the respective configurations [18]. The radial discharge stream from the Std-C is characterized by Kelvin-Helmholtz instability which directs the same towards the tank wall with a small upward inclination from the impeller centre-plane [19]. Whereas, the Low-C might be developing different instabilities which weakens the discharge stream as well as generates additional strong vortices below the impeller which deflects the impeller stream towards the tank bottom. This aspect needs further studies using the advanced experimental and CFD methods.

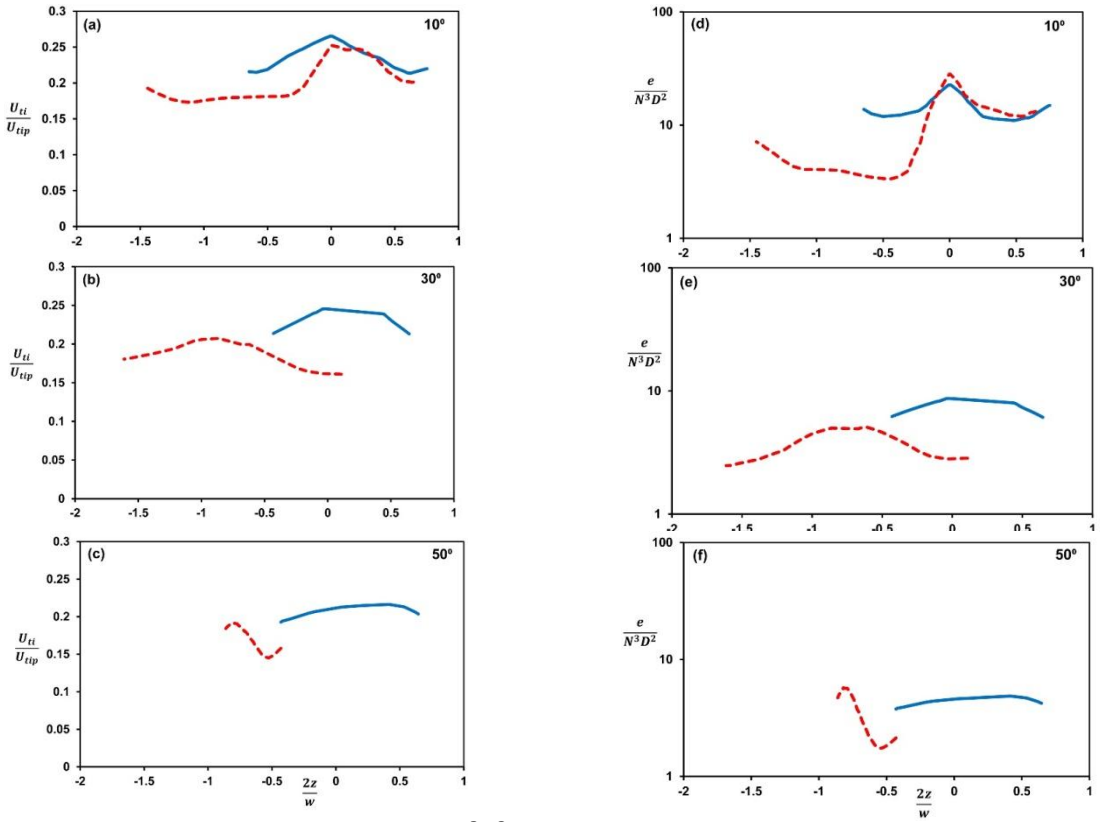


**Fig. 5. Axial profiles of $U_{ti}/U_{tip}$ ((a)-(c)) and $e/N^3D^2$ ((d)-(e)) along the vortex cores at 10°, 30° and 50° behind the blades of Std-C and Low-C. ——: Std-C, – – –: Low-C**

## V. CONCLUSIONS

The steady state CFD approach can be reliably used for modelling the complex flow pattern transition as well as the associated reduction in the power number of the baffled vessels agitated by the RT impeller at Std-C and Low-C respectively. The characteristics of the trailing vortices (such as size, strength and coherency) were drastically diminished from the Std-C to Low-C leading to the reduction in the entrainment of the wake region and strength of the discharge stream behind the impeller blades. The weaker entrainment of the wake results in the reduction of pressure drag and impeller torque which in turn decreases the impeller power number. The significant turbulent action near the bottom of the tank associated with the Low-C is mainly due to the presence of additional strong vortices rather than that contributed by the respective weaker trailing vortices. The weaker discharge stream as well as the additional strong vortices related with the Low-C may be attributed due to the development of new flow instabilities which are different from the Std-C leading to the transition of double loop to single loop re-circulation pattern. This aspect needs detailed exploration in the future using the advanced experimental as well as unsteady RANS and LES methods respectively.

## REFERENCE


[1]. Q. Zhu, H. Xiao, A. Chen, S. Geng, and Q. Huang, "CFD study on double- to single-loop flow pattern transition and its influence on macro mixing efficiency in fully baffled tank stirred by a Rushton turbine",Chi. J. of Chem. Eng., 27:993-1000, 2019.

[2]. A. Ochieng, M. S. Onyango, A. Kumar, K. Kiriamiti, and P. Musonge, "Mixing in a tank stirred by a Rushton turbine at a low clearance",Chem. Eng. Process., 47(5):842-851, 2008.

[3]. G. Montante, K. C. Lee, A. Brucato, and M. Yianneskis, "An Experimental Study of Double-to-Single-Loop Transition in Stirred Vessels",The Can. J. Chem. Eng., 77:649-659, 1999.

[4]. P. M. Armenante, and E. U. Nagamine, "Effect of low off-bottom impeller clearance on the minimum agitation speed for complete suspension of solids in stirred tanks",Chem. Eng. Sci., 53(9):1757-1775, 1998.

[5]. S. Ibrahim, and A. W. Nienow, "Power Curves and Flow Patterns for a Range of Impellers in Newtonian Fluids: $40 < Re < 5x10^{5"}$,Trans. IChemE., 73(A):485-491, 1995.

[6]. Z. Li, Y. Bao, and Z. Gao, "PIV experiments and large eddy simulations of single-loop flow fields in Rushton turbine stirred tanks",Chem. Eng. Sci., 66:1219-1231, 2011.

[7]. G. Montante, K. C. Lee, A. Brucato, and M. Yianneskis, "Experiments and Predictions of the Transition of the Flow Pattern with Impeller Clearance in Stirred Tanks",Chem. Eng. Sci., 56:3751-3770, 2001.

[8]. H. Wu, and G. K. Patterson, "Laser-Doppler Measurements of Turbulent-Flow Parameters in a Stirred Mixer", Chem. Eng. Sci., 44:2207–2221, 1989.

[9]. B. E. Launder, and D. B. Spalding, "The numerical computation of turbulent flows",Comput. Methods Appl. Mech. Eng., 3:269-289, 1974.

[10]. J. Y. Luo, R. I. Issa, and A. D. Gosman."Prediction of impeller induced flows in mixing vessels using multiple frames of reference", Proceedings of the Eighth Eur. Conf. Mix., Instititon of Chemical Engineers Symposium Series, pp. 549-556, 1994.

[11]. I. B. Celik, U. Ghia, P. J. Roache, C. J. Freitas, H. Coleman, and P.E. Raad, "Procedure for Estimation and Reporting of Uncertainty Due to Discretization in CFD Applications",J. Fluids Eng., 130:1-4, 2008.

[12]. J. B. Joshi, N. K. Nere, C. V. Rane, B. N. Murthy, C. S. Mathpati, A. W. Patwardhan, and V. V. Ranade, "CFD simulation of stirred tanks: comparison of turbulence models. Part i: Radial flow impellers" The Can. J. Chem. Eng., 89:23-82, 2011.

[13]. R. L. Bates, P. L. Foundy, and R. R. Corpstein, "Examination of Some Geometric Parameters of Impeller Power", I & EC Process Des. Dev., 2(4):310-314, 1963.

[14]. M. Coroneo, G. Montante, A. Paglianti, and F. Magelli, "CFD Prediction of Fluid Flow and Mixing in Stirred Tanks: Numerical Issues about the RANS Simulations",Comput. Chem. Eng., 35:1959-1968, 2011.

[15]. Y. Huang and M. A. Green, "Detection and tracking of vortex phenomena using Lagrangian coherent structures",Exp. Fluids., 56(147):1-12, 2015.

[16]. R. Escudie, D. Bouyer, and A. Line, "Characterization of Trailing Vortices Generated by a Rushton Turbine",AIChE J., 50(1):75-86, 2004.

[17]. K. Steiros, P. J. K. Bruce, O. R. H. Buxton, and J. C. Vassilicos, "Effect of blade modifications on the torque and flow field of radial impellers in stirred tanks",Phy. Rev. Flu., 2(9):1-20, 2017.

[18]. H. Schulz, A. Simoes, and R. Lobosco (Eds.), Hydrodynamics-Advanced Topics, IntechOpen, Europe and China, 2011.

[19]. C. Bartels, M. Breuer, and F. Durst, "Comparison between direct numerical simulation and k-ε prediction of the flow in a vessel stirred by a Rushton turbine",Proceedings of the 10th European Conference on Mixing, pp. 239-246, 2000.